

Characterization of Impact Toughness of 304L Stainless Steel Fabricated through Laser Powder Bed Fusion Process

Sreekar Karnati¹, Atoosa Khiabani¹, Aaron Flood¹, Frank Liou¹, Joseph W. Newkirk²

¹Department of Mechanical and Aerospace Engineering, Missouri University of Science and Technology, Rolla, MO 65409

²Department of Materials Science and Engineering, Missouri University of Science and Technology, Rolla, MO 65409

Abstract

In this research, the impact toughness of powder bed based additively manufactured 304L stainless steel was investigated. Charpy specimens were built in vertical, horizontal and inclined (45°) orientations to investigate the variation in toughness with build direction. These specimens were tested in as-built and machined conditions. A significant difference in toughness was observed with varying build directions. The lowest toughness values were recorded when the notch was oriented in line with the interlayer boundary. The highest toughness was recorded when the notch was perpendicular to the interlayer boundary. A significant scatter in toughness values was also observed. The variation and distribution among the toughness values were modeled by performing 3-parameter Weibull fits. The performance and variation of the additively manufactured 304L were also compared with the toughness values of wrought 304 stainless. The additively manufactured material was observed to be significantly less tough and more variant in comparison to wrought material.

Introduction

Additive manufacturing (AM) in recent times has risen from being a solely prototyping technology to a full-scale manufacturing technology. Especially for metals, various commercial solutions based on blown powder and powder bed methodologies have been developed to address the demands of the industry. Multiple vendors such as Renishaw, Concept Laser, SLM Solutions, EOS, etc. have developed robust solutions capable of fabricating complex geometries from multiple alloys. Popular alloys such as SS304, Inconel alloys, titanium alloys, precipitation hardenable steels etc. are currently being incorporated into these machines. Despite using similar chemistries as feedstocks, in comparison to conventional processes, parts with drastically different properties are obtained through AM. Such strong differences in material behavior currently limit wide scale incorporation of AM into various industries.

Multiple studies have been performed on comparing the properties of AM material with conventionally fabricated counterparts. The strength properties of AM material have been reported to be similar if not better than their counterparts. However, the properties of AM material were often noticed to be anisotropic. Conclusions from these studies indicate strong direction dependence in mechanical performance [1–13]. The directional heat transfer and rapid solidification in AM process result in a very orderly and repetitive constitution. This type of structure within the AM material is expected produce direction dependent performance.

Yang *et. al.* reported anisotropic tensile performance in Ti6Al4V fabricated through laser powder bed fusion. The directional dependence was attributed to the crystallographic constitution of the material. This anisotropy was also observed to change with input energy density [12]. Chlebus *et. al.* also reported anisotropy in powder bed fabricated Ti6Al7Nb. While strengths higher than conventionally fabricated material were reported, lower ductility and directionally varying performance were also noted [11]. Similar observations in AM fabricated stainless steels were also reported by Suryawanshi *et. al.*[8], Deev *et. al.*[9], and Zhukov *et. al.* [1]. The identification and characterization of such differences are vital to designers. Knowledge of anisotropy is critical for designing structural components. In order to achieve safe and reliable performance, appropriate compensations are necessary to account for the variable properties.

In the current work, the variation of impact toughness with build direction was characterized for powder bed fabricated 304L stainless steel. Impact testing of specimens in as-built and machined conditions was performed. The performance of AM stainless steel was compared against that of wrought material. The scatter in the toughness performance of both materials was also modeled.

Experimental setup

The AM material in the current study was fabricated using the Renishaw AM250 machine located at Missouri S&T. The parameters used to fabricate the specimens for the study were optimized for attaining maximum density and high quality downward facing surfaces. The Renishaw machine follows a point-by-point exposure method as opposed to a continuous laser scan which is typical for most laser based powder bed machines. During this point by point exposure, a power of 200W, a point spacing of 65 micron, an exposure time of 75 micro seconds and a hatch spacing of 85 micron were used. The chemistry of the powder used for AM fabrication is listed in Table 1. For the comparative study, a 7/16” wrought 304 stainless steel bar stock (rolled and annealed) was also analyzed. The composition of the wrought material is listed in Table 2.

Table 1. The chemical composition of 304L stainless steel powder

Element	C	Cr	Cu	Fe	Mn	N	Ni	O	P	S	Si
Wt. %	0.018	18.4	< 0.1	Bal	1.4	0.06	9.8	0.02	0.012	0.005	0.6

Table 2. The chemical composition of wrought 304L stainless steel bar stock

Element	C	Cr	Cu	Fe	Mn	N	Ni	O	P	S	Si
Wt. %	0.03	18-20	-	Bal	2	0.01	8-12	-	0.045	0.03	1

The Charpy specimens were prepared to a size of 55mmx10mmx10mm. The 2mm deep “V” notch was machined using a standard broach. Two sets of AM specimens were built for Charpy testing. These specimens were built in vertical, horizontal and 45° orientations. A screenshot of the build layout is shown in Figure 1. The two sets of specimens were prepared for testing in as-built and machined conditions (). The specimens were built in the same layout for

both of the surface conditions. The specimens for testing in the machined state were built oversized to account for the machining compensation. For comparison, specimens made from wrought stainless steel were also tested. The wrought raw stock was machined to dimensions and notched for testing. The total number of specimens tested in each case are shown in Table 3.

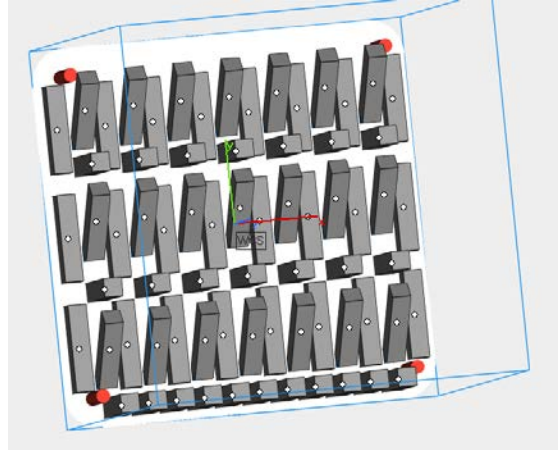


Figure 1: Build layout for Charpy specimens in different orientations, XY directions along the plate Z direction same as the build direction (out of the paper).

Table 3: Total number of specimens tested for impact toughness.

Material	Orientation	# of specimens
SLM, As-built	0	23
	45	20
	90	25
SLM, Machined	0	24
	45	21
	90	24
Wrought	Notch perpendicular to the rolling direction	30

Results and Discussions

The densities of the machined AM specimens measured by Archimedes method in distilled water, categorized by build orientation are shown in Figure 2. While there was no statistically significant difference in densities, the variance and median values for each orientation were observed to be different. The variance among the specimens built along the build direction was observed to be the highest. The median density of the 45 degrees specimens was the highest and vertical specimens was the lowest. The large density variance in vertical specimens is suspected to be due to the difference in probability of formation of lack of fusion defects. While the parameters were optimized for maximum density, several environmental factors (humidity,

oxygen entry during powder feed, inconsistency in wiper setup etc.) can influence the probability of pore formation and in extension the part density. The specimens built in the vertical orientation require the highest number of layers for completion of fabrication and hence can contain large variance in density. The density is also influenced by the build location, lens transmission deterioration (accumulation of condensed metal, ejecta, fines etc.).

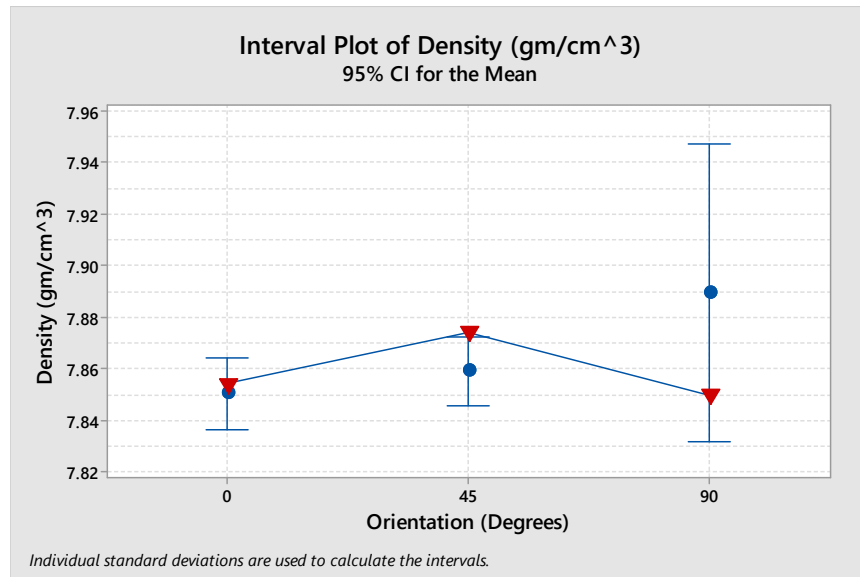


Figure 2: Density values of machined specimens built in 0, 45, and 90-degree orientations with respect to the substrate. ‘●’ is the mean and ‘▼’ is the median, the connecting line joins the medians, the error bars span a range of 2 standard deviations.

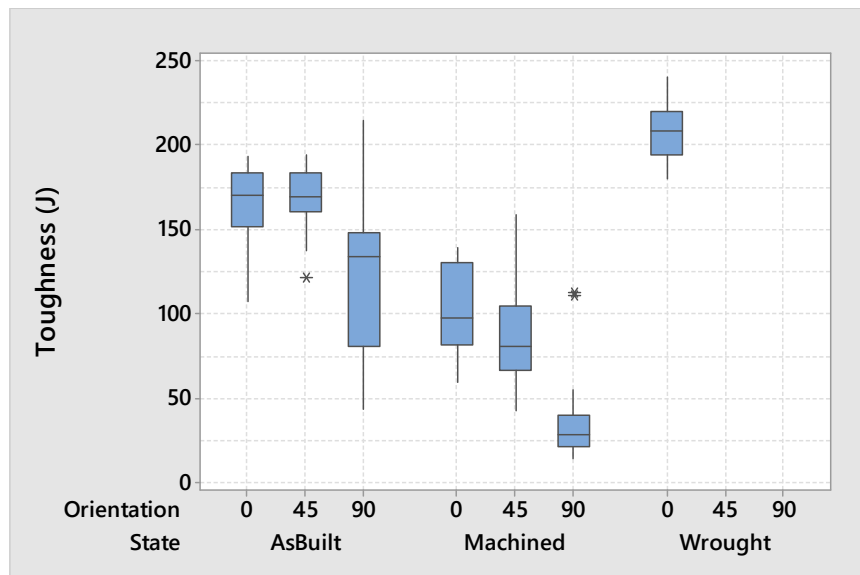


Figure 3: Box plot of toughness values measured from AM specimens in as-built and machined states and wrought specimens.

For specimens tested in both as-built and machined state, the toughness values of the specimens built vertically were substantially lower than those of horizontal and 45-degree specimens. The toughness values of 45-degree specimens were observed to be slightly lower when tested in the machined state. However, the difference was observed to be insignificant when tested in the as-built state. The same can be seen from the box plots shown in Figure 3. Overall the toughness values of specimens in as-built conditions were observed to be substantially higher than those of machined condition. This observation is counter-intuitive, the poor surface quality is expected to result in early failure and lower toughness. This difference in toughness is suspected to be an artifact of the differences in the testing of as-built and machined specimens.

While the as-built specimens were designed to be built to size, they are consistently oversized from the specification (by approx. 0.1mm). Although this difference is small, it is still consistent. This small difference in material volume could add to the toughness value of the as-built specimen. The surface quality between these specimens is also dramatically different. The as-built specimens have a rough finish which is an artifact of the build process, whereas the machined specimens have a smooth finish. The difference in friction can add to the toughness of the as-built specimens. Also noticeably different plastic deformation was observed in the regions where the specimens come in contact with the pins (See Figure 4). The as-built specimens underwent more deformation in comparison to the machined specimens leading to extra energy absorption and high toughness measurements.

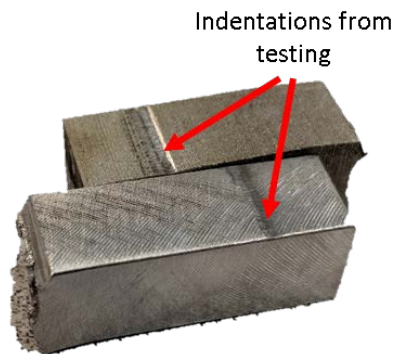


Figure 4: Difference in plastic deformation from indentation of the pins during Charpy testing (red arrows). Larger deformation on as-built specimens in comparison to machined specimens

Three parameter Weibull fits of the toughness data was performed to model the variation in toughness with orientation and material type [14]. The equation of the three-parameter Weibull distributions is as follows,

$$P(x) = \left(\frac{m}{\beta}\right) \left(\frac{x - \theta}{\beta}\right)^{m-1} \exp \left[-\left(\frac{x - \theta}{\beta}\right)^m \right], x > 0, \theta > 0$$

Where P is the probability of event the occurring, x is the random variable (impact toughness in this case), m is the Weibull modulus or shape parameter, β is the scale or characteristic value and θ is the threshold value. Weibull modulus or the shape parameter describes the breadth of the

distribution. The threshold value is an estimate of the value under which the probability of the event occurring is zero. From a designer’s perspective, the threshold value is the most critical input. Basing the threshold value as the failure criteria, maximum life and performance can be reliably expected from a component. The Weibull fits of data from machined and wrought specimens are shown in Figure 5. The values of the Weibull parameters are shown in Figure 6 .

Similar to the conclusions from the box plots in Figure 3, Weibull representation also indicates the variation in vertical samples was substantially higher than the remaining orientations (see Figure 5). The lowest toughness value in the vertical orientation is substantially smaller than those in horizontal and inclined orientation. The performance from the inclined orientation is slightly inferior to that of the horizontal orientation. However, the scatter in the performance is similar. The drastic differences in the threshold values indicate the need for considering material anisotropy during component design.

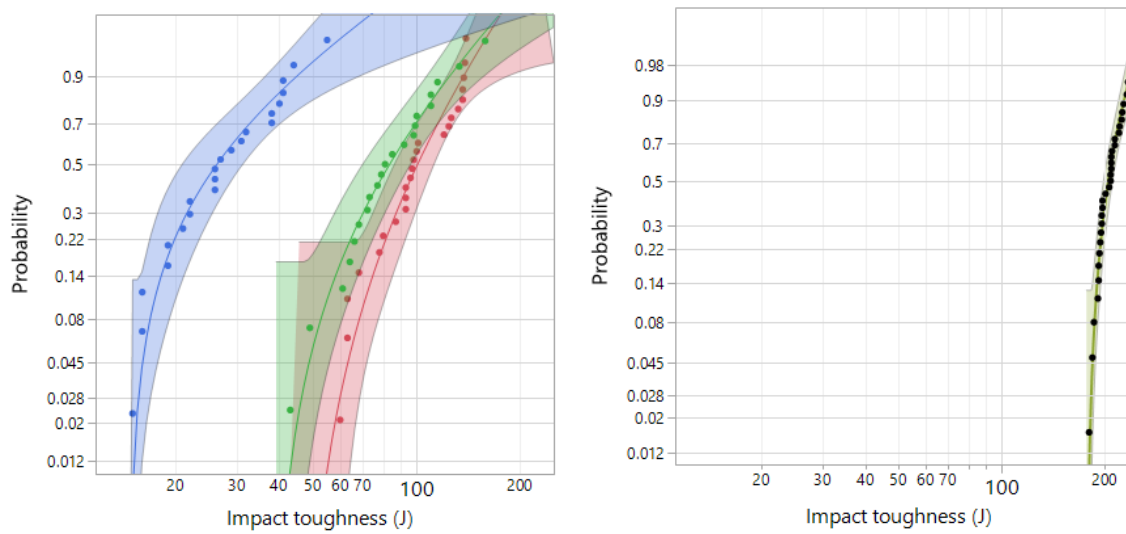


Figure 5: Three parameter Weibull fits of toughness data for powder bed (left) and wrought (right) 304 stainless steel.

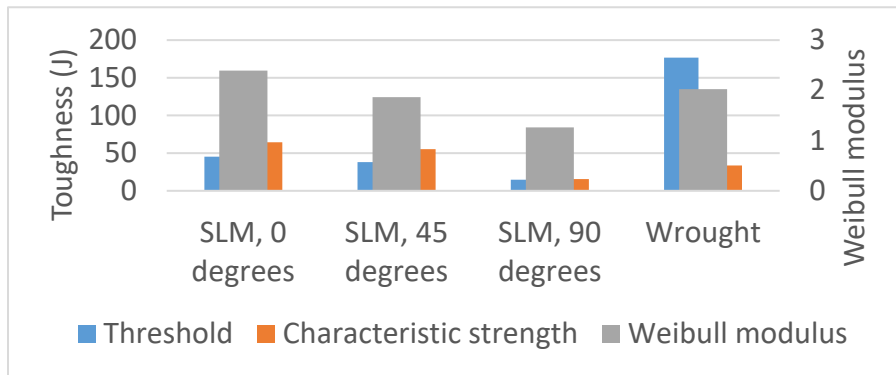


Figure 6: Summary of Weibull parameters from the fits shown in Figure 5.

The threshold values of AM material were substantially lower than those of wrought material. While the Weibull modulus of wrought material was lower than the Weibull modulus of horizontal AM specimens, the difference between the threshold and characteristic strength were substantially different for the horizontal AM specimens. The Weibull modulus values were observed to decrease with orientation for the AM specimens, 0 degrees was the highest and 90 degrees was the lowest. Overall, the AM material performance is significantly inferior and scattered in comparison to wrought material.

In order to understand the anisotropy and the inferior performance of AM material, the fracture surfaces of the broken Charpy specimens were investigated. The fracture surfaces of the specimens with lowest, median and highest toughness values were imaged using ASPEX SEM. The complete stitched images of the fracture surfaces are shown in Figure 7.

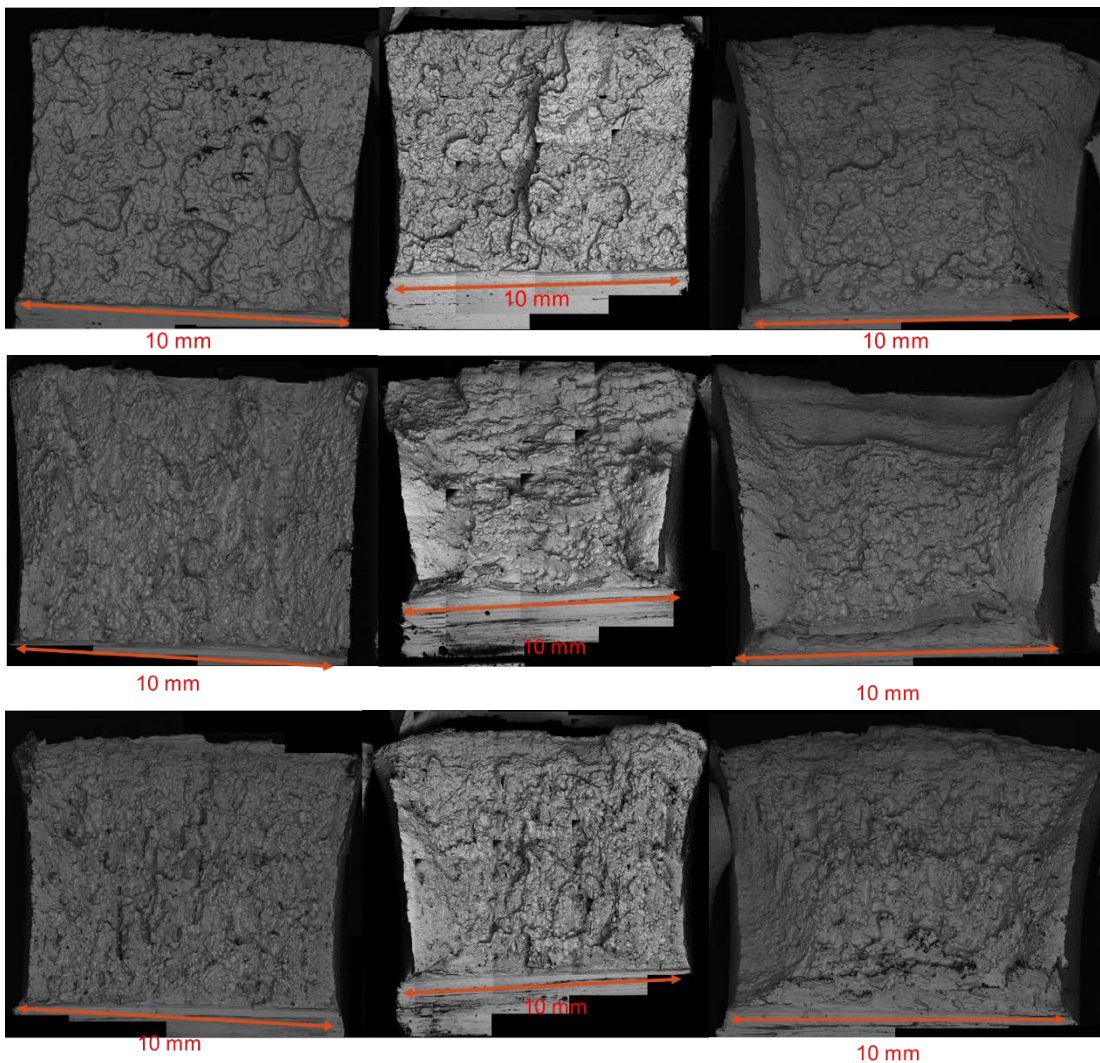


Figure 7: Stitched images of fracture surfaces of specimens with lowest (left column), median (middle column) and highest (right column) values of toughness in vertical (top row), 45 degrees (middle row) and horizontal (bottom row) orientations.

The toughness values of the specimens are in agreement with the deformation of the cross-section. The lowest performers have a near zero deformation of the cross section, suggesting a brittle failure. Whereas the best performers have significant deformations indicating ductile failure. The vertical specimen with the lowest toughness value in comparison to the horizontal specimens with both lowest and highest toughness value has a near square cross-section suggesting minimal amounts of deformation. The lack of deformation and low toughness value could be indicative of a failure mechanism whose sensitivity varies with build orientation. While dimples, representative of ductile failure, were present across the fracture surface, features in the shape of smoothly rounded pits were also observed (see Figure 8). The shape of these pits was observed to vary with orientation. From the shape and size of these features, these pits appear to be track boundaries. This could imply that the weakest link in this AM material could be track boundaries. Furthermore, the large variance and low toughness of vertical specimens could mean that the inter-layer track boundary is the weakest link in the AM material.

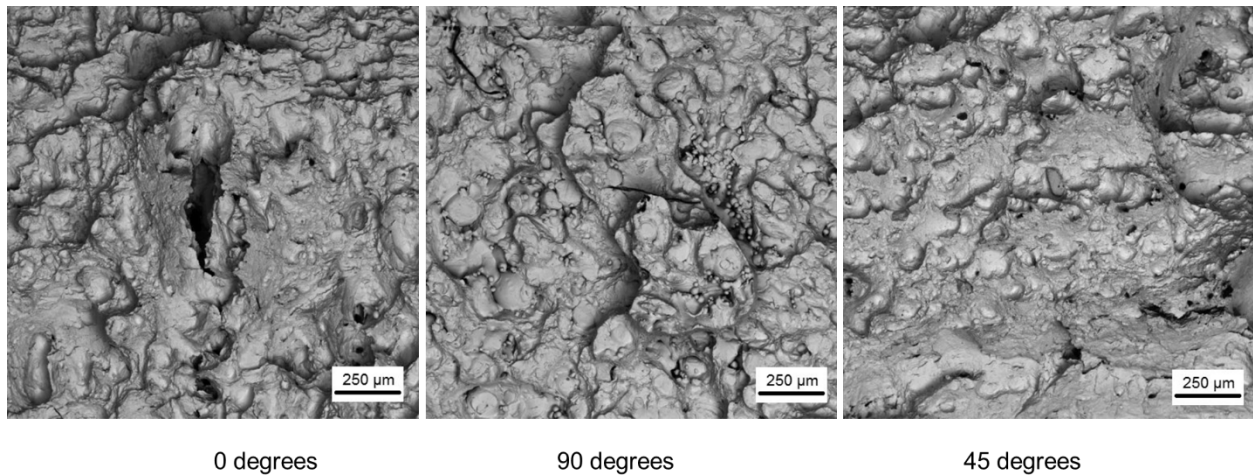


Figure 8: Close up images of fracture surfaces of horizontal, vertical and 45 degrees specimens with median toughness values.

Macro images of fracture surfaces from broken Charpy specimens are shown in Figure 9. From the figure, it can again be observed that the fracture surfaces possess an atypical pattern for ductile materials. Features such as steps, grooves, and ridges can be seen on the fracture surface. Especially, the fracture surface of the vertically built specimens indicates sharp changes in the direction of crack propagation. The step-like features are expected from 90 degree turns in the direction of crack propagation. The step-like features could be a result of the joining of cracks initiated in different layers.

If the “V” notch is in between layers (vertical samples), step-like features were observed. If the notch is perpendicular/inclined to the interlayer boundary, grooves/ ridges have been observed. Considering the location of the notch and the patterns on the fracture surfaces, the propagation of the crack is expected to be exclusively along the interlayer boundary.



Figure 9: Fracture surfaces of broken Charpy specimens built in different build orientations.

To confirm the above claims, cross sections of broken specimens were cut, ground, polished and etched to reveal the microstructure (shown in Figure 10). The microstructure along the fracture surface substantiates the above claims. The fracture surface was seen to be along the track/interlayer boundary. The step-like features were formed due to the changes in the direction of crack propagation from one interlayer boundary to another along the track boundaries in between those two sets of layers. The difference in build orientations causes a difference in location of the notch with respect to the interlayer boundaries. This makes the vertical specimens the most susceptible and the horizontal specimens the most resistant to failure. This also explains the difference in the type of patterns observed on the fracture surface.

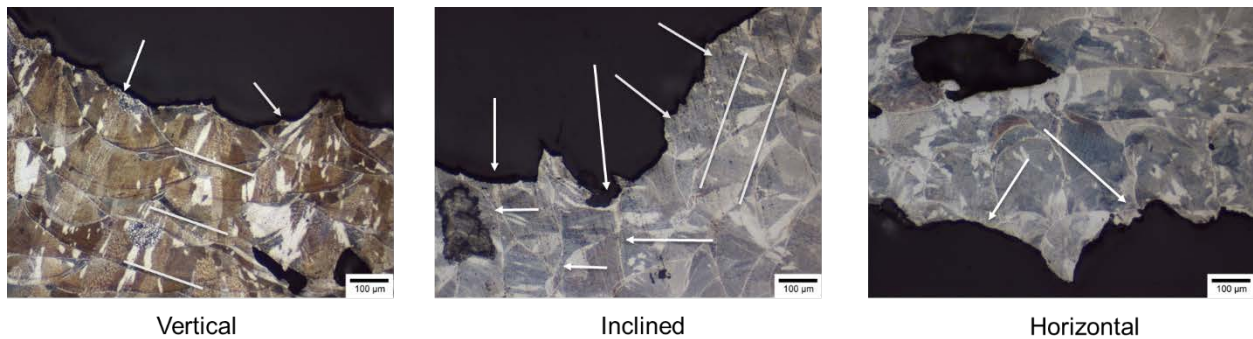


Figure 10: Microstructure along the fracture surface on a plane normal to the notch on broken specimens

The low performance of the AM material despite high densities and the atypical crack propagation along the track boundaries implies the presence of a critical flaw along the track boundaries. The ordered and repetitive constitution of AM material also orders the said flaw throughout the fabricated component. Upon loading, the performance of the AM material is dependent on the access of the crack to this flaw distribution. While the presence of the flaw was not identifiable under low magnification imaging, further investigation is required to explore this failure mechanism.

Conclusions

- The impact performance of AM 304L stainless steel material fabricated using laser powder bed fusion was studied against that of wrought 304L stainless steel.
- While the specimens had high densities, the performance of the AM material was inferior to that of wrought material.
- A substantial amount of anisotropy in impact toughness was observed with varying build direction. The vertically built specimens exhibited the lowest toughness performance.
- The scatter in the toughness performance of the vertically built specimens was also substantially higher than that of the other two build orientations.
- The fracture surfaces of the broken specimens indicate an atypical failure pattern for ductile materials.
- The crack propagation was exclusively along the track boundary. The varying access of the crack to the interlayer track boundary was identified to be the source of anisotropy.

Acknowledgments

This work has been funded by Honeywell Federal Manufacturing & Technologies under Contract No. DE-NA0002839 with the U.S. Department of Energy. The United States Government retains and the publisher, by accepting the article for publication, acknowledges that the United States Government retains a nonexclusive, paid up, irrevocable, world-wide license to publish or reproduce the published form of this manuscript, or allow others to do so, for the United States Government purposes. The supports from National Science Foundation Grants CMMI-1625736, and the Intelligent Systems Center (ISC) at Missouri S&T are greatly appreciated.

Furthermore, the authors would like to acknowledge Kyle Stagner, Ian Wille, and Brian Bullock for their aid in this research.

References

- [1] A. Zhukov, A. Deev, P. Kuznetsov, Effect of Alloying on the 316L and 321 Steels Samples Obtained by Selective Laser Melting, *Phys. Procedia*. 89 (2017) 172–178. doi:10.1016/J.PHPRO.2017.08.010.
- [2] Y.M. Wang, T. Voisin, J.T. McKeown, J. Ye, N.P. Calta, Z. Li, Z. Zeng, Y. Zhang, W. Chen, T.T. Roehling, R.T. Ott, M.K. Santala, P.J. Depond, M.J. Matthews, A. V. Hamza, T. Zhu, Additively manufactured hierarchical stainless steels with high strength and ductility, *Nat. Mater.* 17 (2017) 63–71. doi:10.1038/nmat5021.
- [3] V. Cain, L. Thijs, J. Van Humbeeck, B. Van Hooreweder, R. Knutsen, Crack propagation and fracture toughness of Ti6Al4V alloy produced by selective laser melting, *Addit. Manuf.* 5 (2015) 68–76. doi:10.1016/J.ADDMA.2014.12.006.
- [4] B. Van Hooreweder, D. Moens, R. Boonen, J.-P. Kruth, P. Sas, Analysis of Fracture Toughness and Crack Propagation of Ti6Al4V Produced by Selective Laser Melting, *Adv. Eng. Mater.* 14 (2012) 92–97. doi:10.1002/adem.201100233.
- [5] M.-W. Wu, P.-H. Lai, J.-K. Chen, Anisotropy in the impact toughness of selective laser

©2018 The Department of Energy's Kansas City National Security Campus is operated and managed by Honeywell Federal Manufacturing Technologies, LLC under contract number DE-NA0002839.

- melted Ti–6Al–4V alloy, *Mater. Sci. Eng. A.* 650 (2016) 295–299.
doi:10.1016/J.MSEA.2015.10.045.
- [6] I. Tolosa, F. Garcíandía, F. Zubiri, F. Zapirain, A. Esnaola, Study of mechanical properties of AISI 316 stainless steel processed by “selective laser melting”, following different manufacturing strategies, *Int. J. Adv. Manuf. Technol.* 51 (2010) 639–647.
doi:10.1007/s00170-010-2631-5.
- [7] E. Liverani, S. Toschi, L. Ceschini, A. Fortunato, Effect of selective laser melting (SLM) process parameters on microstructure and mechanical properties of 316L austenitic stainless steel, *J. Mater. Process. Technol.* 249 (2017) 255–263.
doi:10.1016/J.JMATPROTEC.2017.05.042.
- [8] J. Suryawanshi, K.G. Prashanth, U. Ramamurty, Mechanical behavior of selective laser melted 316L stainless steel, *Mater. Sci. Eng. A.* 696 (2017) 113–121.
doi:10.1016/J.MSEA.2017.04.058.
- [9] A.A. Deev, P.A. Kuznetsov, S.N. Petrov, Anisotropy of Mechanical Properties and its Correlation with the Structure of the Stainless Steel 316L Produced by the SLM Method, *Phys. Procedia.* 83 (2016) 789–796. doi:10.1016/J.PHPRO.2016.08.081.
- [10] D. Kono, A. Maruhashi, I. Yamaji, Y. Oda, M. Mori, Effects of cladding path on workpiece geometry and impact toughness in Directed Energy Deposition of 316L stainless steel, *CIRP Ann.* (2018). doi:10.1016/J.CIRP.2018.04.087.
- [11] E. Chlebus, B. Kuźnicka, T. Kurzynowski, B. Dybała, Microstructure and mechanical behaviour of Ti—6Al—7Nb alloy produced by selective laser melting, *Mater. Charact.* 62 (2011) 488–495. doi:10.1016/J.MATCHAR.2011.03.006.
- [12] J. Yang, H. Yu, Z. Wang, X. Zeng, Effect of crystallographic orientation on mechanical anisotropy of selective laser melted Ti-6Al-4V alloy, *Mater. Charact.* 127 (2017) 137–145. doi:10.1016/J.MATCHAR.2017.01.014.
- [13] M.-W. Wu, P.-H. Lai, The positive effect of hot isostatic pressing on improving the anisotropies of bending and impact properties in selective laser melted Ti-6Al-4V alloy, *Mater. Sci. Eng. A.* 658 (2016) 429–438. doi:10.1016/J.MSEA.2016.02.023.
- [14] Y. Takashima, M. Ohata, F. Minami, Analysis of Statistical Scatter in Charpy Impact Toughness, *Mater. Sci. Forum.* 783–786 (2014) 2394–2399.
doi:10.4028/www.scientific.net/MSF.783-786.2394.